Long-term Stress Distribution Patterns of the Ankle Joint in Varus Knee Alignment Assessed by Computed Tomography Osteoabsorptiometry

Tomohiro Onodera, MD, PhD[1]
Tokifumi Majima, MD, PhD[2]
Norimasa Iwasaki, MD, PhD[1]
Tamotsu Kamishima, MD, PhD[3]
Yasuhiko Kasahara, MD, PhD[1]
Akio Minami, MD, PhD[1]

1. Department of Orthopaedic Surgery
Hokkaido University Graduate School of Medicine
North 15 West 7, Kita-ku, Sapporo 060-8638
Japan

2. Department of Joint Replacement and Tissue Engineering
Hokkaido University Graduate School of Medicine
North 15 West 7, Kita-ku, Sapporo 060-8638
Japan

3. Department of Biomedical Science and Engineering
Hokkaido University Hospital
North 15 West 7, Kita-ku, Sapporo 060-8638
Japan

Please address all correspondence to:

Tomohiro Onodera, MD., PhD.
Department of Orthopaedic Surgery
Hokkaido University Graduate School of Medicine
North 15 West 7, Kita-ku, Sapporo 060-8638, Japan
Tel.: (+81)-11-706-5935; Fax: (+81)-11-706-6054
Email: tomozou@med.hokudai.ac.jp

Abstract

Purpose: The stress distribution of an ankle under various physiological conditions is important for long-term survival of total ankle arthroplasty. The aim of this study was to measure subchondral bone density across the distal tibial joint surface in patients with malalignment/instability of the lower limb.

Methods: We evaluated subchondral bone density across the distal tibial joint in patients with malalignment/instability of the knee. Subchondral bone density of the ankle was measured by computed tomography (CT) osteoabsorptiometry from ten ankles as control and from 27 ankles with varus deformity/instability of the knee. The quantitative analysis focused on the location of the high-density area at the articular surface, to determine the resultant long-term stress on the ankle joint.

Results: The area of maximum density of subchondral bone was located in the medial part in all subjects. The pattern of maximum density in the anterolateral area showed stepwise increases with the development of varus deformity/instability of the knee.

Conclusions: Our results should prove helpful for designing new prostheses and determining clinical indications for total ankle arthroplasty.

Keywords: *Computed tomography, CT osteoabsorptiometry, total ankle arthroplasty, varus knee*

Introduction

Ankle osteoarthritis (OA) is not uncommon in patients with malalignment of the mechanical axis of the lower limb[1] or tibial malalignment after fractures.[2,3] Malalignment of the lower limb may thus accelerate the degenerative change in ankle joint. Although malalignment of the lower limb often occurs due to OA of the knee, the prevalence of primary OA has been reported as uncommon compared with other OA.[4,5]

This discrepancy is thought to have several causes, such as anatomical congruency, composition of the extracellular matrix, and biomechanical condition.[6,7] The natural ankle joint offers high resistance against mechanical stress. Even recent prostheses for total ankle arthroplasty do not display survival comparable to that with total hip or knee arthroplasty.[8,9] One reason for this short survival is considered to be coronal plane deformity. The relationship between clinical outcomes and preoperative coronal alignment of the ankle joint is well established, but malalignment of the lower limb that could dynamically affect the ankle joint is not currently given sufficient consideration for total ankle arthroplasty.[10,11]

Extensive in vitro investigations have reported on ankle articular cartilage biomechanics using cadaveric experimental setups.[12,13] Recent in vivo studies have also attempted to quantify articular cartilage contact biomechanics in the ankle joint.[14,15] The results have been crucially important in the design of recent prostheses and determining clinical indications for total ankle arthroplasty. However, no studies have investigated effects on the articular surface of the ankle joint in lower limb malalignment/instability. Load-bearing conditions and

variations in lower limb alignment may complicate evaluation of the pathological ankle joint.

To overcome such difficulties, we tried to investigate subchondral bone density of the ankle joint by computed tomography (CT) osteoabsorptiometry. The distribution of subchondral bone density reflects the stress pattern of a joint under long-term physiological conditions.[16,17] CT osteoabsorptiometry can assess long-term stress distribution at individual joints in living subjects by measuring subchondral bone density. Previous studies using this method have evaluated stress distribution at each joint under various loading scenarios, from normal to pathological or postoperative conditions.[18-22] Clarification of the distribution pattern of ankle subchondral bone density in patients with malalignment of the lower limb may provide insights into the design of novel implants for ankle arthroplasty and the determination of clinical indications for ankle arthroplasty.

The aim of this study was to measure subchondral bone density across the distal tibial joint surface in patients with malalignment of the lower limb by CT osteoabsorptiometry. The results obtained indicate the influence of lower limb malalignment on stress distributions in the ankle joint.

Methods

Data collection

Institutional review board approval was obtained prior to initiation of this study. CT image data were obtained from 27 women who underwent CT-based navigation for total knee arthroplasty. No patients had any symptoms in the ankle or history of significant ankle trauma. The control group comprised 5 volunteers (10 ankles) with no history of knee or ankle injury. Sample size was based on a power analysis using data from our pilot study and previous

investigations.[20,23,24] These studies showed a 0.09-point target difference in mean value of the high-density area ratio described below (effect size) and a standard deviation less than 0.03 points. Power analysis indicated that at least 5 subjects would be required to detect this effect size with 90% power and a significance of $\alpha = 0.05$. We therefore used the current study design with a minimum sample size of 8 subjects.

Kellgren and Lawrence (K/L) grades for patients with medial compartment knee OA were determined based on radiographic data and all patients were evaluated as K/L grade 3 or 4. The mechanical axis was defined as the angle between a line from the center of the hip to the mid-point of the ankle joint, and was assessed on full-length standing radiographs. The femoro-tibial angle, formed by the union of the mechanical axes of the femur and tibia and an angle exceeding 176 degrees is considered to represent a varus deformity, was measured in weight-bearing radiographs and categorized into one of four subgroups: control group, mean femoro-tibial angle 174.2 degrees (n=10; mean age, 36.8 years; 95% CI, 35.1 to 38.5); moderate group, femoro-tibial angle 185 degrees or less (n=9; mean age, 73.5 years; 95% CI, 70.5 to 76.5); severe group, femoro-tibial angle more than 185 degrees (n=10; mean age, 74.4 years; 95% CI, 69.0 to 79.8); and thrust group, clinical observation of lateral thrust, as sideways movement of the knee in the early stance phase of gait[25,26] (n=8; mean age, 69.8 years; 95% CI, 65.0 to 74.5) (Table 1). Determination of mechanical axes was performed from full-limb weight-bearing radiographs. We performed all digital measurements and calculations using CentricityWeb-J 3.0 HD software (GE Healthcare Japan, Tokyo, Japan). Ankle joints showing narrowing of the joint space on standing radiography were excluded. Patients showing ankle joint pain or instability were also excluded. No significant differences in age or body mass index (BMI) were noted among the

three groups.

CT osteoabsorptiometry

The obtained imaging data were transferred to an image analyzing system (Advantage Windows; GE Medical Systems, Milwaukee, MI) for further evaluation. Coronal views at intervals of 1 mm were reconstructed from the obtained CT images. The subchondral bone region of the distal articular surface of the tibia, as the target area for measurement, was automatically identified using original software (OsteoDens 4.0). In each slice, X-ray attenuation (in Hounsfield units (HU), whereby water is 0 and compact bone is 1000) of the identified subchondral bone region was measured at each coordinate point with 1-mm intervals (Fig. 1). For each subject, the range between maximum and minimum HU values was divided into nine equal grades, and a surface mapping image depicted by the nine grade color scale was created. The technical details of CT osteoabsorptiometry have been described previously.[20,16,22]

Data analysis

Quantitative analysis of the obtained mapping data focused on the location of the area of maximum density in the entire articular surface. [20,24,22] The area of maximum density was defined as the area in which HU values were >600 HU (nine grade color scale). The percentage of the maximum density area (%MA) at each divided region of the tibial articular surface was calculated and statistically compared among the four groups. The divided regions included the antero-medial part (ant-med), postero-medial part (post-med), antero-lateral part (ant-lat), and postero-lateral part (post-lat) (Fig. 2). The %MA in each region was defined as the area of maximum density divided by the total articular area for that region. Before

the analysis for each group, intraobserver consistency in the measurement of mechanical axes, femoro-tibial angle on radiographs, and subchondral bone density was assessed by calculating the coefficient of variation (CV), as the standard deviation divided by the mean value. For this assessment, the investigator performed five measurements of the same CT image. CVs for %MA were calculated from five sets of results.

Statistical analysis

Statistical comparisons among the three groups were conducted using analysis of variance (ANOVA) and Fisher's protected least-significant difference test. Differences were considered significant for only p values less than 0.05.

Results

Consistency of the Analytical Method

CVs of measurement for mechanical axes, femoro-tibial angle on radiographs, and %MA for the entire distal surface of the tibia by a single observer were 2.3%, 1.8%, and 2.6%, respectively. Variation less than 10% was considered acceptable for comparative study purposes. To reduce data variation, measurements in this study were all performed by the same investigator.

Data Analysis

For all subjects in the control group, almost the entire area of maximum density was found in the ant-med and post-med areas (Table 2, Fig. 3A). The %MAs for ant-med and post-med were significantly higher than in other regions ($p < 0.05$).

For all subjects in the moderate knee OA group, the area of maximum density was predominantly found in the ant-med and post-med areas (Fig. 3B).

The %MAs for ant-med and post-med were significantly higher than in other regions ($p < 0.05$).

All subjects in the severe group demonstrated a higher density area widely distributed in the ant-lat area, compared to that in the control and moderate group (Fig. 3C). The %MA for ant-med was significantly higher than for ant-lat or post-lat ($p < 0.05$).

In the thrust group, high-density areas were increased in the ant-lat without decreasing in the medial area (Fig. 3D). The %MA of the ant-med was significantly higher than in ant-lat and post-lat regions ($p < 0.05$).

Regarding the results of comparisons of %MA among the four groups, values in the ant-lat and post-lat areas increased in a stepwise manner from the control group to the moderate, severe, and thrust groups. In the ant-lat area, the %MA of severe and thrust groups was significantly higher than that of the control group ($p < 0.05$). The %MA of the thrust group for post-lat was also significantly higher than that for the control group ($p < 0.05$).

Discussion

Contact area and intraarticular pressure in the ankle joint have mostly been studied using in-vitro cadaveric ankle specimens[27-32] and finite element models.[33,34] Despite various in-vitro studies, measurement of in-vivo intraarticular pressure in the ankle joint remains a challenge in the field of biomedical engineering. Most analyses on activities of daily living such as weight-bearing standing or gait have been unable to predict the long-term physiological condition of the ankle joint. CT osteoabsorptiometry can be used to clarify subchondral bone density. The theoretical background for this method is that subchondral bone mineralization functionally adapts to repeated and long-

term changes in joint loading.[12] Elucidation of mineralization patterns thus allows investigators to predict mechanical conditions in joints. The obtained results indicate alterations in stress distributions through the ankle joint in living subjects.

The current analysis demonstrated that the area of maximum density for subchondral bone across the articular surface of the tibia was located in the antero-medial part in all subjects. The area of maximum density was significantly decreased in the severe knee OA group compared to the control and moderate OA group. These results indicate that actual stress across the articular surface of the distal tibia is located in the medial part under conditions of normal alignment and moderate varus deformity of the knee joint, whereas stress distribution in the ankle joint shifts from medial to anterolateral in the severely varus deformed knee. Instability (thrust knee) also shifts stress anterolaterally, but medial stress was also increased compared to that in the control group.

A recent study was able to show contact areas on both articular surfaces using dual fluoroscopic and magnetic resonance imaging techniques.[15] That study showed that contact areas were mainly distributed in lateral regions during the simulated stance phase of walking. However, our results show that subchondral bone density in the medial part was obviously higher than that in the lateral part. Their study could clarify aspects of total activity of daily life at a just one time point, whereas our results reflect long-term physiological stress on the ankle, including walking stress. The cause of discrepancies between our results and those of that previous study may be that CT osteoabsorptiometry reflects the dynamic stress pattern of a joint under long-term physiological conditions.

Some autopsy studies have demonstrated that a quarter or one-third of knee OA patients show OA in the ankle joint.[35,36] Tallroth et al. retrospectively examined the coexistence of ankle OA and knee OA, finding that 30 of 104

patients with knee OA also showed ankle OA.[1] They also stated that preoperative femoro-tibial angle and mechanical axis deviation are strongly correlated with the grade of ankle OA. These results support our findings for imbalance stress areas in knee OA patients. Theoretically, the increase in varus knee deformity should induce medial stress in the ankle joint. However, our results from the severe knee OA group showed a decrease in bone mineralization at the anteromedial part of the tibia compared with the moderate knee OA group. This result may be attributable to compensation for the alignment of the subtalar joint. To confirm this speculation, future analyses using CT osteoabsorptiometry should be directed toward the detailed analysis of other subjects.

In this study, the following considerations must be kept in mind. First, the obtained results were based on indirect measurement of stress acting on the ankle joint. Absolute values of joint stress were not clarified here. Second, a significant discrepancy in age existed between the control group and other groups. While control group should ideally match other groups in age, age-matched samples with no history of knee and ankle pain or injury are extremely difficult to obtain. To better understand the biomechanical conditions of the ankle in varus knee deformity, more CT data need to be collected from elder groups with normal knee alignment. Third, we did not take into account factors such as walking aids, vitamin D values, and foot alignment. These factors might have influenced the results. Finally, stress distributions across a joint are mainly determined by loading conditions and joint geometry. Although this study showed relationships between stress distributions and long-term loading conditions through the ankle joint, the effects of ankle geometry on stress distribution should be clarified. Although the present study includes these limitations, the results still offer a basic

clarification of the relationship between in vivo stress distributions in the ankle joint and lower limb alignment.

In conclusion, significant alterations in the distribution of subchondral bone density across the distal articular surface of the tibia were found among the four groups with different levels of varus knee deformity/instability. Instability of the knee increases stress in all parts of the ankle. Varus malalignment of the knee without instability increases stress in the antero-lateral part of the ankle without increasing stress in the medial part, providing valuable information for the design of novel implants for the ankle and for determining clinical indications for total ankle arthroplasty. Furthermore, the present results may indicate that total ankle arthroplasty in patients with knee deformity/instability may carry a risk of loosening because of shifts in stress distribution when knee deformity/instability is not corrected.

Conflict of interest statement: The authors declare that they have no conflict of interest.

References

1. Tallroth K, Harilainen A, Kerttula L, Sayed R (2008) Ankle osteoarthritis is associated with knee osteoarthritis. Conclusions based on mechanical axis radiographs. Arch Orthop Trauma Surg 128 (6):555-560. doi:10.1007/s00402-007-0502-9

2. Merchant TC, Dietz FR (1989) Long-term follow-up after fractures of the tibial and fibular shafts. J Bone Joint Surg Am 71 (4):599-606

3. van der Schoot DK, Den Outer AJ, Bode PJ, Obermann WR, van Vugt AB (1996) Degenerative changes at the knee and ankle related to malunion of tibial fractures. 15-year follow-up of 88 patients. J Bone Joint Surg Br 78 (5):722-725

4. Saltzman CL, Salamon ML, Blanchard GM, Huff T, Hayes A, Buckwalter JA, Amendola A (2005) Epidemiology of ankle arthritis: report of a consecutive series of 639 patients from a tertiary orthopaedic center. Iowa Orthop J 25:44-46

5. Valderrabano V, Horisberger M, Russell I, Dougall H, Hintermann B (2009) Etiology of ankle osteoarthritis. Clin Orthop Relat Res 467 (7):1800-1806. doi:10.1007/s11999-008-0543-6

6. Gunther KP, Sturmer T, Sauerland S, Zeissig I, Sun Y, Kessler S, Scharf HP, Brenner H, Puhl W (1998) Prevalence of generalised osteoarthritis in patients with advanced hip and knee osteoarthritis: the Ulm Osteoarthritis Study. Ann Rheum Dis 57 (12):717-723

7. Treppo S, Koepp H, Quan EC, Cole AA, Kuettner KE, Grodzinsky AJ (2000) Comparison of biomechanical and biochemical properties of cartilage from human knee and ankle pairs. J Orthop Res 18 (5):739-748. doi:10.1002/jor.1100180510

8. Gougoulias N, Khanna A, Maffulli N (2010) How successful are current ankle replacements?: a systematic review of the literature. Clin Orthop Relat Res 468 (1):199-208. doi:10.1007/s11999-009-0987-3

9. Stengel D, Bauwens K, Ekkernkamp A, Cramer J (2005) Efficacy of total ankle replacement with meniscal-bearing devices: a systematic review and meta-analysis.

Arch Orthop Trauma Surg 125 (2):109-119. doi:10.1007/s00402-004-0765-3

10. Doets HC, Brand R, Nelissen RG (2006) Total ankle arthroplasty in inflammatory joint disease with use of two mobile-bearing designs. J Bone Joint Surg Am 88 (6):1272-1284. doi:88/6/1272 [pii]

10.2106/JBJS.E.00414

11. Wood PL, Sutton C, Mishra V, Suneja R (2009) A randomised, controlled trial of two mobile-bearing total ankle replacements. J Bone Joint Surg Br 91 (1):69-74. doi:91-B/1/69 [pii]

10.1302/0301-620X.91B1.21346

12. Koepp H, Eger W, Muehleman C, Valdellon A, Buckwalter JA, Kuettner KE, Cole AA (1999) Prevalence of articular cartilage degeneration in the ankle and knee joints of human organ donors. J Orthop Sci 4 (6):407-412. doi:90040407.776 [pii]

13. Muehleman C, Margulis A, Bae WC, Masuda K (2010) Relationship between knee and ankle degeneration in a population of organ donors. BMC Med 8:48. doi:1741-7015-8-48 [pii]

10.1186/1741-7015-8-48

14. Li G, Wan L, Kozanek M (2008) Determination of real-time in-vivo cartilage contact deformation in the ankle joint. J Biomech 41 (1):128-136. doi:S0021-9290(07)00314-4 [pii]

10.1016/j.jbiomech.2007.07.006

15. Wan L, de Asla RJ, Rubash HE, Li G (2006) Determination of in-vivo articular cartilage contact areas of human talocrural joint under weightbearing conditions. Osteoarthritis Cartilage 14 (12):1294-1301. doi:S1063-4584(06)00161-0 [pii]

10.1016/j.joca.2006.05.012

16. Muller-Gerbl M, Putz R, Hodapp N, Schulte E, Wimmer B (1989) Computed tomography-osteoabsorptiometry for assessing the density distribution of subchondral bone as a measure of long-term mechanical adaptation in individual joints. Skeletal Radiol 18 (7):507-512

17. Muller-Gerbl M, Putz R, Hodapp N, Schulte E, Wimmer B (1990) [Demonstration of subchondral density pattern using CT-osteoabsorptiometry (CT-OAM) for the

assessment of individual joint stress in live patients]. Z Orthop Ihre Grenzgeb 128 (2):128-133. doi:10.1055/s-2008-1039487

18. Eckstein F, Lohe F, Muller-Gerbl M, Steinlechner M, Putz R (1994) Stress distribution in the trochlear notch. A model of bicentric load transmission through joints. J Bone Joint Surg Br 76 (4):647-653

19. Eckstein F, Muller-Gerbl M, Steinlechner M, Kierse R, Putz R (1995) Subchondral bone density in the human elbow assessed by computed tomography osteoabsorptiometry: a reflection of the loading history of the joint surfaces. J Orthop Res 13 (2):268-278. doi:10.1002/jor.1100130215

20. Iwasaki N, Minami A, Miyazawa T, Kaneda K (2000) Force distribution through the wrist joint in patients with different stages of Kienbock's disease: using computed tomography osteoabsorptiometry. J Hand Surg Am 25 (5):870-876. doi:S0363-5023(00)51508-1 [pii]

10.1053/jhsu.2000.16353

21. Muller-Gerbl M, Weisser S, Linsenmeier U (2008) The distribution of mineral density in the cervical vertebral endplates. Eur Spine J 17 (3):432-438. doi:10.1007/s00586-008-0601-5

22. Oizumi N, Suenaga N, Minami A, Iwasaki N, Miyazawa T (2003) Stress distribution patterns at the coracoacromial arch in rotator cuff tear measured by computed tomography osteoabsorptiometry. J Orthop Res 21 (3):393-398. doi:S0736026602002310 [pii]

10.1016/S0736-0266(02)00231-0

23. Makabe H, Iwasaki N, Kamishima T, Oizumi N, Tadano S, Minami A Computed tomography osteoabsorptiometry alterations in stress distribution patterns through the wrist after radial shortening osteotomy for Kienbock disease. J Hand Surg Am 36 (7):1158-1164. doi:S0363-5023(11)00476-X [pii]

10.1016/j.jhsa.2011.04.001

24. Momma D, Iwasaki N, Oizumi N, Nakatsuchi H, Funakoshi T, Kamishima T, Tadano S, Minami A (2011) Long-Term Stress Distribution Patterns Across the Elbow Joint in Baseball Players Assessed by Computed Tomography Osteoabsorptiometry.

Am J Sports Med 39 (2):336-341. doi:0363546510383487 [pii]
10.1177/0363546510383487
25. Ogata K, Yasunaga M, Nomiyama H (1997) The effect of wedged insoles on the thrust of osteoarthritic knees. Int Orthop 21 (5):308-312
26. Scott WN (2006) Examination of the knee. In: INSALL and SCOTT Surgery of the Knee
fourth edition edn. Churchill Livingstone, Elsevier, Philadelphia,
27. Christensen JC, Driscoll HL, Tencer AF (1994) 1994 William J. Stickel Gold Award. Contact characteristics of the ankle joint. Part 2. The effects of talar dome cartilage defects. J Am Podiatr Med Assoc 84 (11):537-547
28. Driscoll HL, Christensen JC, Tencer AF (1994) Contact characteristics of the ankle joint. Part 1. The normal joint. J Am Podiatr Med Assoc 84 (10):491-498
29. Michelson JD, Checcone M, Kuhn T, Varner K (2001) Intra-articular load distribution in the human ankle joint during motion. Foot Ankle Int 22 (3):226-233
30. Ramsey PL, Hamilton W (1976) Changes in tibiotalar area of contact caused by lateral talar shift. J Bone Joint Surg Am 58 (3):356-357
31. Steffensmeier SJ, Saltzman CL, Berbaum KS, Brown TD (1996) Effects of medial and lateral displacement calcaneal osteotomies on tibiotalar joint contact stresses. J Orthop Res 14 (6):980-985. doi:10.1002/jor.1100140619
32. Wagner KS, Tarr RR, Resnick C, Sarmiento A (1984) The effect of simulated tibial deformities on the ankle joint during the gait cycle. Foot Ankle 5 (3):131-141
33. Anderson DD, Goldsworthy JK, Li W, James Rudert M, Tochigi Y, Brown TD (2007) Physical validation of a patient-specific contact finite element model of the ankle. J Biomech 40 (8):1662-1669. doi:S0021-9290(07)00072-3 [pii]
10.1016/j.jbiomech.2007.01.024
34. Reggiani B, Leardini A, Corazza F, Taylor M (2006) Finite element analysis of a total ankle replacement during the stance phase of gait. J Biomech 39 (8):1435-1443. doi:S0021-9290(05)00178-8 [pii]
10.1016/j.jbiomech.2005.04.010
35. Buckwalter JA, Saltzman CL (1999) Ankle osteoarthritis: distinctive

characteristics. Instr Course Lect 48:233-241

36. Huch K, Kuettner KE, Dieppe P (1997) Osteoarthritis in ankle and knee joints. Semin Arthritis Rheum 26 (4):667-674. doi:S0049-0172(97)80002-9 [pii]

Figure legends

Table 1. Patient demographics. Values represent mean (±standard deviation). OA, osteoarthritis; BMI, body mass index (weight in kilograms divided by the square of the height in meters). *P < 0.05 vs. other groups.

Table 2. Mean percentage (%) of the maximum density area of each region in the four groups. Values represent mean (±standard deviation).*P < 0.05 vs. post-lat area in all areas. **P < 0.05 vs. ant-lat area and vs. post-lat area in all areas. †P < 0.05 vs. control group in all groups. Ant-med, anteromedial region; Post-med, posteromedial region; Ant-lat, anterolateral region; Post-lat, posterolateral region.

Figure 1: Quantitative analysis by computed tomography (CT) osteoabsorptiometry. Distribution of the subchondral bone density is obtained by stacking data, including Hounsfield unit value at each coordinate point **(a)**. The distribution pattern is presented as a surface mapping image depicted in a nine-grade color scale **(b)**.

Figure 2: Three-dimensional computed tomography (3D-CT) view of the tibial articular surface from the sole of the foot. Divided regions for quantitative analysis of the obtained mapping data: ant-med, anteromedial region; post-med,

posteromedial region; ant-lat, anterolateral region; post-lat, posterolateral region. Representative case was chosen as the sample in which the percentage maximum areas in the four areas were close to the mean values of moderate group.

Figure 3: Results of computed tomography (CT)-osteoabsorptiometry. Representative results for CT osteoabsorptiometry and comparison of mean percentages of the maximum density area (%MA) for each region between groups (**A**, control group; **B**, moderate group; **C**, severe group; **D**, thrust group). **D)** Data are shown as mean ± standard error of the mean (SEM). *P < 0.05 vs. post-lat area. **P < 0.05 vs. ant-lat area and vs. post-lat area. Ant-med, anteromedial region; Post-med, posteromedial region; Ant-lat, anterolateral region; Post-lat, posterolateral region.

	Age (years)	Weight (kg)	BMI	Mechanical axis (%)	Lateral femorotibial angle (°)
Moderate group	73.5 [70.5 to 76.5]	62.7 [56.5 to 68.8]	27.3 [25.9 to 28.7]	89.5 [80.0 to 99.0]	181.9 [181.2 to 182.6]
Severe group	74.4 [69.0 to 79.8]	62.0 [54.5 to 69.5]	27.4 [24.2 to 30.6]	120.7* [110.4 to 130.0]	191.4* [188.5 to 194.3]
Thrust group	69.8 [65.0 to 74.5]	63.6 [57.0 to 70.3]	27.2 [24.2 to 30.2]	93.0 [81.9 to 104.1]	184.4 [181.0 to 187.9]
Control group	36.8* [35.1 to 38.5]	54.2* [50.5 to 57.9]	22.1* [21.1 to 23.2]	50.2* [48.4 to 52.0]	174.2* [173.4 to 175.0]

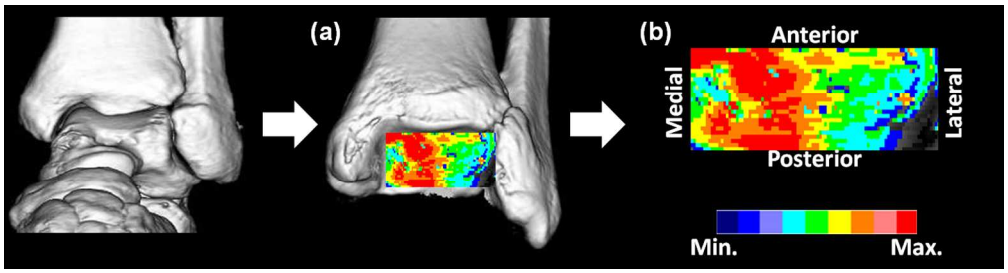

254x66mm (150 x 150 DPI)

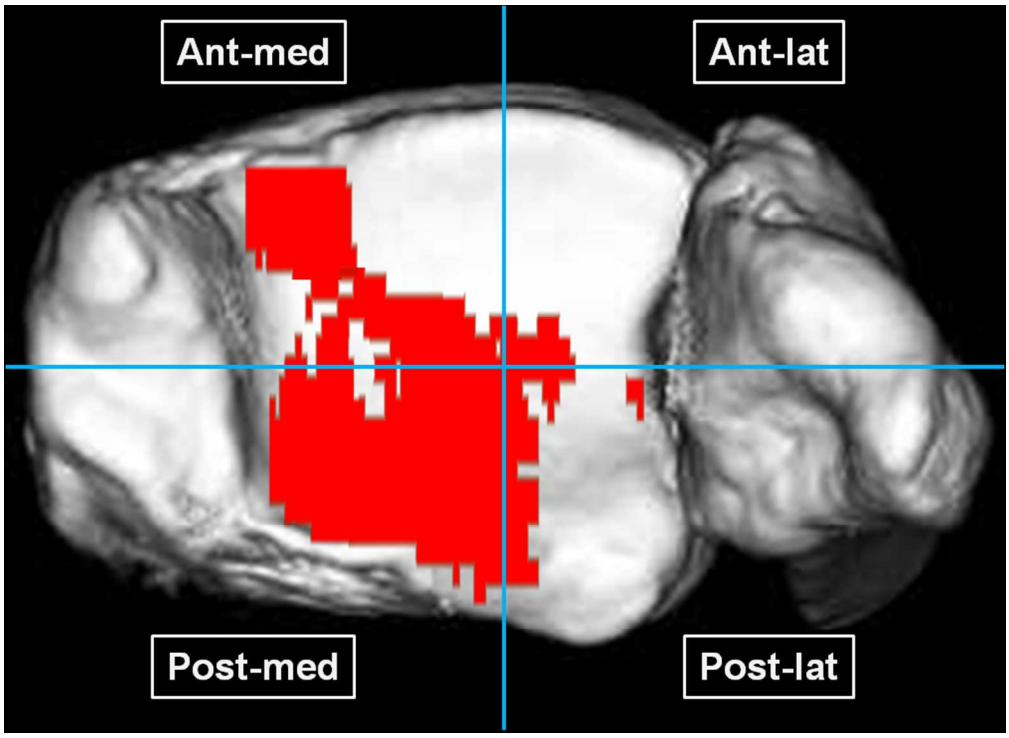

170x123mm (150 x 150 DPI)

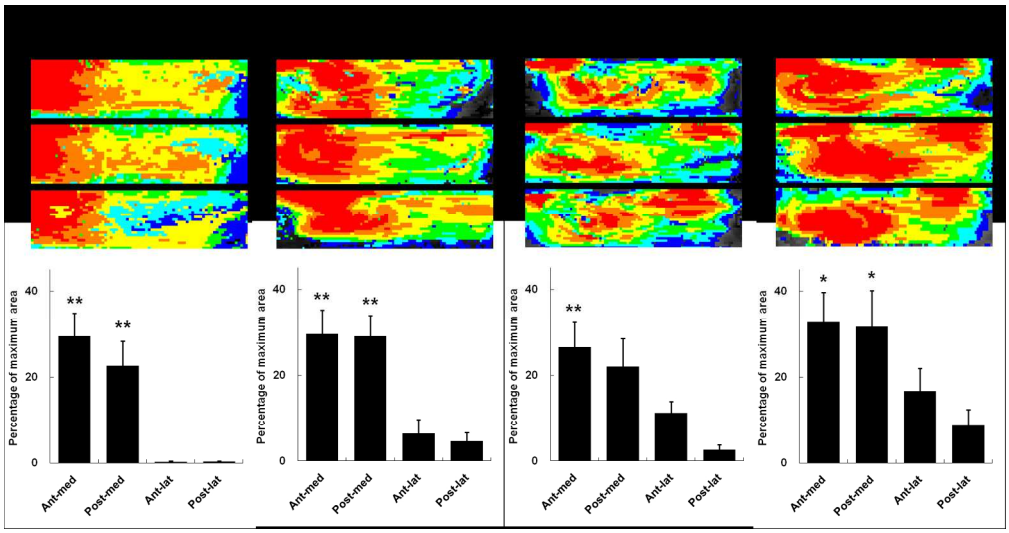

377x196mm (150 x 150 DPI)

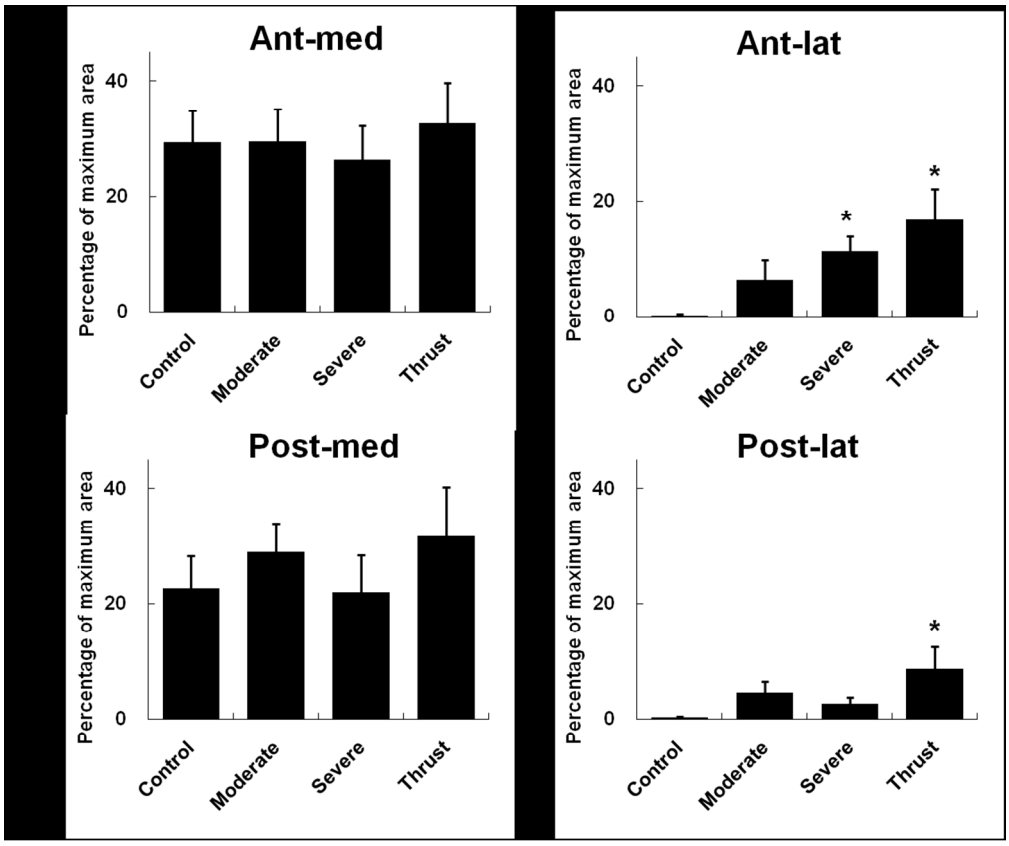

213x178mm (150 x 150 DPI)